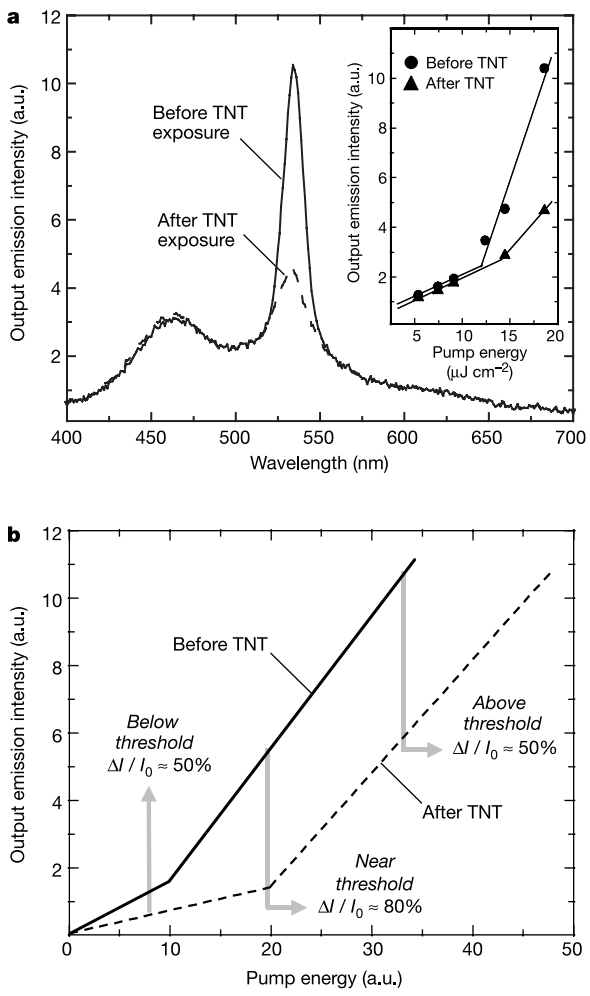

Figure 4 Response of a ring-mode laser coated with polymer **1**. **a**, Spectral response of a ring-mode structure consisting of a 25-μm diameter silica fibre dip-coated with a polymer **1** thin film. ASE attenuation in the absence of spontaneous emission attenuation after 1.5 min exposure to saturated TNT vapour pressure. Inset, plots of ASE peak emission intensity ($\lambda = 535$ nm) as a function of excitation power. TNT exposure increases the pump energy threshold. **b**, A general sketch of the ASE E_{TH} increase after exposure of the SOP film to a quencher such as TNT. The change in the output emission intensity divided by the initial output emission intensity, I/I_0, is largest at pump energies just below the E_{TH} of analyte-exposed films.

increases, which results in a quenching signal of larger magnitude. Unfortunately, with longer operating times (>1 min), the higher excitation power can lead to photobleaching, which interferes with the quenching response. Nevertheless, in instances where the greatest amount of signal is required, one may achieve this through increasing the excitation power, which shortens the operating lifetime of the active polymer film.

The strong binding of the nitroaromatic analytes DNT and TNT to electron-rich SOPs and their ease of reduction makes for a selective response that is relatively immune to interference[6,18], and no response was observed upon exposure of our devices to benzene or naphthalene. Current and future efforts focus on incorporating SOPs into high-Q optical feedback structures that will allow further reduction in E_{TH} as well as an enhanced sensitivity with reduced thickness of the active layer. □

Received 28 April 2004; accepted 4 February 2005; doi:10.1038/nature03438.

1. Zhou, Q. & Swager, T. M. Methodology for enhancing the sensitivity of fluorescent chemosensors: energy migration in conjugated polymers. *J. Am. Chem. Soc.* **117,** 7017–7018 (1995).
2. Swager, T. M. The molecular wire approach to sensory signal amplification. *Acc. Chem. Res.* **31,** 201–207 (1998).
3. McQuade, D. T., Pullen, A. E. & Swager, T. M. Conjugated polymer-based sensory materials. *Chem. Rev.* **100,** 2537–2574 (2000).
4. Tessler, N., Denton, G. J. & Friend, R. H. Lasing from conjugated-polymer microcavities. *Nature* **382,** 695–697 (1996).
5. Yang, J.-S. & Swager, T. M. Porous shape persistent fluorescent polymer films: An approach to TNT sensory materials. *J. Am. Chem. Soc.* **120,** 5321–5322 (1998).
6. Cumming, C. J. *et al.* Using novel fluorescent polymers as sensory materials for above-ground sensing of chemical signature compounds emanating from buried landmines. *IEEE Trans. Geosci. Remote Sens.* **39,** 1119–1128 (2001).
7. Rose, A., Lugmair, C. G. & Swager, T. M. Excited-state lifetime modulation in triphenylene-based conjugated polymers. *J. Am. Chem. Soc.* **123,** 11298–11299 (2001).
8. Zahn, S. & Swager, T. M. Three-dimensional electronic delocalization in chiral conjugated polymers. *Angew. Chem. Int. Edn Engl.* **41,** 4225–4230 (2002).
9. Kozlov, V. G., Bulović, V., Burrows, P. E. & Forrest, S. F. Laser action in organic semiconductor waveguide and double heterostructure devices. *Nature* **389,** 362–365 (1997).
10. Bulović, V., Kozlov, V. G., Khalfin, V. B. & Forrest, S. R. Transform-limited, narrow-linewidth lasing action in organic semiconductor microcavities. *Science* **279,** 553–555 (1998).
11. Scherf, U., Riechel, S., Lemmer, U. & Mahrt, R. F. Conjugated polymers: lasing and stimulated emission. *Curr. Opin. Solid State Mater. Sci.* **5,** 143–154 (2001).
12. Halls, J. J. M., Pichler, K., Friend, R. H., Moratti, S. C. & Holmes, A. B. Exciton diffusion and dissociation in a poly(*p*-phenylenevinylene)/C_{60} heterojunction photovoltaic cell. *Appl. Phys. Lett.* **68,** 3120–3122 (1996).
13. Hamer, P. J. *et al.* Optical studies of chemical doping achieved by ion implantation in poly(p-phenylene vinylene). *Phil. Mag. B* **73,** 367–382 (1996).
14. Levitsky, I. A., Kim, J. & Swager, T. M. Energy migration in a poly(phenylene ethynylene): determination of interpolymer transport in anisotropic Langmuir-Blodgett films. *J. Am. Chem. Soc.* **121,** 1466–1472 (1999).
15. Kogelnik, H. & Shank, C. V. Stimulated emission in a periodic structure. *Appl. Phys. Lett.* **18,** 152–154 (1971).
16. Heliotis, G. *et al.* Emission characteristics and performance comparison of polyfluorene lasers with one- and two-dimensional distributed feedback. *Adv. Funct. Mater.* **14,** 91–97 (2004).
17. Berggren, M., Dodabalapur, A., Slusher, R. E. & Bao, Z. Light amplification in organic thin films using cascade energy transfer. *Nature* **389,** 466–469 (1997).
18. Yang, Y.-S. & Swager, T. M. Fluorescent porous polymer films as TNT chemosensors: electronic and structural effects. *J. Am. Chem. Soc.* **120,** 11864–11873 (1998).

Supplementary Information accompanies the paper on **www.nature.com/nature**.

Acknowledgements This work was supported by NASA, the Institute for Soldier Nanotechnologies, and the NSF through the Center for Materials Science and Engineering. A.R. acknowledges V. Sundar and H. Eisler for discussions and J. Ho for providing the DFB structures used in this work.

Competing interests statement The authors declare that they have no competing financial interests.

Correspondence and requests for materials should be addressed to T.M.S. (tswager@mit.edu) or V.B. (bulovic@mit.edu).

Light-induced shape-memory polymers

Andreas Lendlein[1,2], Hongyan Jiang[2,3], Oliver Jünger[2]* & Robert Langer[4]

[1]*GKSS Research Center Geesthacht GmbH, Institute of Chemistry, Kantstraβe 55, D-14513 Teltow, Germany*
[2]*Institute for Technology and Development of Medical Devices, RWTH Aachen, Pauwelsstraβe 30, and* [3]*mnemoScience GmbH, Pauwelsstraβe 19, D-52074 Aachen, Germany*
[4]*Department of Chemical Engineering, Massachusetts Institute of Technology, 45 Carleton Street, Cambridge, Massachusetts 02139, USA*

* Present address: Prof.-Staudinger-Strasse, D-65451 Kelsterbach, Germany

Materials are said to show a shape-memory effect if they can be deformed and fixed into a temporary shape, and recover their original, permanent shape only on exposure to an external stimulus[1–3]. Shape-memory polymers have received increasing attention because of their scientific and technological significance[4,5]. In principle, a thermally induced shape-memory effect can be activated by an increase in temperature (also obtained by heating on exposure to an electrical current[6] or light illumination[6,7]). Several papers have described light-induced changes in

the shape of polymers[8–12] and gels[13–15], such as contraction[8–10], bending[11–13] or volume changes[14,15]. Here we report that polymers containing cinnamic groups can be deformed and fixed into pre-determined shapes—such as (but not exclusively) elongated films and tubes, arches or spirals—by ultraviolet light illumination. These new shapes are stable for long time periods, even when heated to 50 °C, and they can recover their original shape at ambient temperatures when exposed to ultraviolet light of a different wavelength. The ability of polymers to form different pre-determined temporary shapes and subsequently recover their original shape at ambient temperatures by remote light activation could lead to a variety of potential medical and other applications.

As an example of the shape-memory functionality of such photoresponsive materials, results of programming and recovering induced by light are shown in Fig. 1. First, a photoresponsive polymer is conventionally processed into its permanent shape, a plain film (Fig. 1A, a). Afterwards, the polymer film is stretched to 20% elongation by external stress, and both sides of the film were evenly irradiated with ultraviolet (UV) light, wavelength $\lambda > 260$ nm, for 60 min. When the external stress is released, the sample stayed in an elongated form (Fig. 1A, b). Irradiating the elongated shape with UV light of $\lambda < 260$ nm for 60 min induces cleaving of newly formed photosensitive crosslinks. As a consequence, the recovery of the memorized, permanent shape, that is, the original length (Fig. 1A, c), is observed. Other temporary shapes can also be produced. For example, when only the top side of a polymer film in a stretched state (100% elongation) is irradiated with UV light of $\lambda > 260$ nm for 60 min, a corkscrew spiral shape is obtained after release of external stress (Fig. 1B). The formation of such a spiral shape is caused by the formation of two layers. While the deformation is well-fixed for the top layer, the bottom layer keeps its elasticity. As a result, the latter contracts much more than the former when the external stress is released, forming an arch or corkscrew spiral shape.

Thermoresponsive shape-memory polymers consist of two components on the molecular level: first, molecular switches, which are segments having a thermal transition at temperature T_{trans} and that fix the temporary shape by forming physical crosslinks; and second, 'netpoints' that link these segments and determine the permanent shape[4]. In photoresponsive shape-memory polymers (Fig. 1C), we want the netpoints to be part of

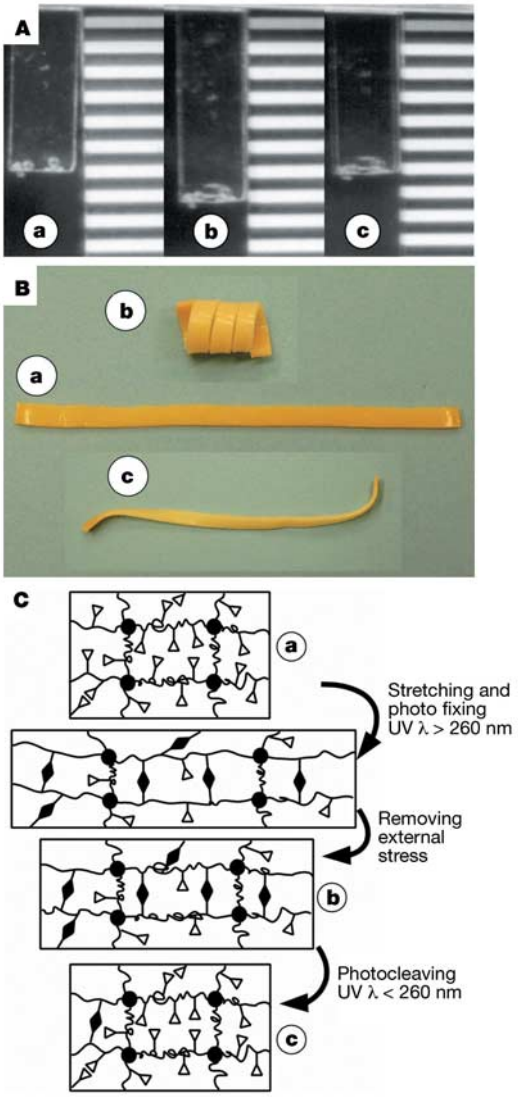

Figure 1 Shape-memory effect of photoresponsive polymers. **A**, A film of grafted polymer BHCA(10,2,1). **a**, Permanent shape (6 cm × 1.2 cm × 0.05 cm); **b**, temporary shape; **c**, recovered permanent shape. **B**, An IPN polymer film. **a**, Permanent shape (8 cm × 0.4 cm × 0.05 cm); **b**, corkscrew spiral temporary shape; **c**, recovered shape obtained by irradiation with UV light of $\lambda < 260$ nm for 60 min. **C**, Molecular mechanism of shape-memory effect of the grafted polymer network: the chromophores (open triangles) are covalently grafted onto the permanent polymer network (filled circles, permanent crosslinks), forming photoreversible crosslinks (filled diamonds); fixation and recovery of the temporary shape are realized by UV light irradiation of suitable wavelengths.

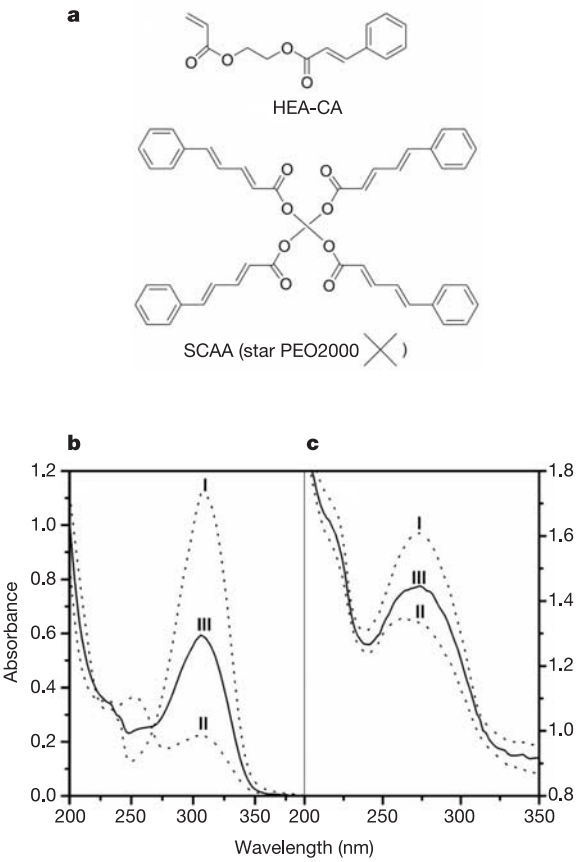

Figure 2 UV absorption spectra. **a**, Chemical structure of molecular switches HEA-CA and SCAA. **b**, A thin film of SCAA. Shown are spectra taken 0 min (spectrum I) and 6 min (II) after exposure to UV light of $\lambda > 260$ nm (crosslinking), and after another 6 min exposure to UV light of $\lambda < 260$ nm (III; de-crosslinking). **c**, A thin film of grafted polymer BHCA(10,2,1): Shown are spectra taken 0 min (I) and 60 min (II) after exposure to UV light of $\lambda > 260$ nm, and after 60 min exposure to UV light of $\lambda < 260$ nm (III).

a covalently crosslinked, amorphous permanent polymer network. The molecular switches are photoresponsive cinnamic acid type molecules such as cinnamic acid (CA)[16] and cinnamylidene acetic acid (CAA)[17], which are able to undergo efficient photoreversible [2 + 2] cycloaddition reactions when exposed to alternating wavelengths (here: $\lambda > 260$ nm or $\lambda < 260$ nm). When such a photoresponsive polymer film (Fig. 1C, a, permanent shape) is stretched, the coiled segments of the amorphous polymer chains between two netpoints are elongated. Upon exposure to UV light of $\lambda > 260$ nm, the elongated segments of the chains are partially fixed owing to formation of new photoresponsive crosslinks, resulting in an elongated new shape (Fig. 1C, b, temporary shape). The photoresponsive crosslinks can be reversibly cleaved by irradiation with UV light of $\lambda < 260$ nm. As a result, the fixed elongated film can recover to the original permanent shape (Fig. 1C, c, recovered permanent shape).

We created two photoresponsive shape-memory polymers. In the first polymer ('grafted polymer'), CA molecules are grafted onto the permanent polymer network, forming a polymer architecture, as schematically illustrated in Fig. 1C. Grafted polymers are obtained by copolymerization of *n*-butylacrylate (BA), hydroxyethyl methacrylate (HEMA) and ethyleneglycol-1-acrylate-2-CA (HEA-CA, in Fig. 2a) with poly(propylene glycol)-dimethacrylate (number-average molecular mass $M_n = 560\ g\ mol^{-1}$, PPG2M560) as crosslinker. Here the molecular switches are photoreversible crosslinks, fixing the deformed temporary shape when irradiated with UV light of $\lambda > 260$ nm, and recovering the shape when exposed to UV light of $\lambda < 260$ nm, as schematically illustrated in Fig. 1C. Only the CA chromophore is selected as a molecular switch, because CAA-containing (meth)acrylates cannot be incorporated into the permanent network via free-radical polymerization. CAA groups may possibly work as free-radical scavengers during the reaction. We synthesized a series of polymer networks with CA groups (Supplementary Table 1). Increasing the amount of HEA-CA increases both the elastic moduli and the glass-transition temperatures (T_g) of the grafted polymer networks, probably owing to the bulky side chains of the CA groups and/or π–π interaction of CA molecules. All polymer networks are amorphous, and have glass-transition temperatures lower than 20 °C.

In the second polymer ('IPN polymer'), the permanent network is formed from BA with 3.0 wt% poly(propylene glycol)-dimethacrylate ($M_n = 1{,}000\ g\ mol^{-1}$, PPG2M1000) as crosslinker. The permanent network was loaded with about 20 wt% star-poly(ethylene glycol) containing CAA terminal groups (SCAA, in Fig. 2a) by swelling it in a 10 wt% SCAA chloroform solution, forming an opaque yellow film (BP-SCAA) after the solvent is removed. Under the influence of light, these SCAA molecules can be reversibly crosslinked, fixing the temporary shape by interpenetrating the permanent network.

Figure 2b shows changes in the absorption spectra of SCAA when exposed to UV light of $\lambda > 260$ nm and UV light of $\lambda < 260$ nm. The absorption maximum at 310 nm (Fig. 2b, spectrum I) relating to conjugated diene groups decreased from 1.1 to 0.2 after 6 min exposure to UV light of $\lambda > 260$ nm (Fig. 2b, spectrum II). At the same time, the absorption peak at 250 nm relating to the formed styryl groups increased. The spectral changes are indicative of the disappearance of the double bonds adjacent to carbonyl groups of the CAA moiety, and the formation of a cyclobutane ring bearing styryl groups. On exposure to UV light of $\lambda < 260$ nm for another 6 min, the formed cyclobutane ring is reversibly cleaved and the absorption peak at 310 nm increases again (Fig. 2b, spectrum III). The extent of photoreversibility is around 40%, which is determined from the intensity changes of the absorption peak at 310 nm. The grafted polymer networks having CA groups show a maximum absorption at 275 nm, and a similar photoreversibility (Fig. 2c).

Unlike azo-containing liquid crystal elastomers[9–13] but similar to polymers having a thermally induced shape-memory effect[2–4], our photosensitive polymers require pre-determined programming—including deformation into a new shape by application of an external force. Irradiating free-standing, non-deformed polymer films did not change their shape. For potential specific applications, different original and deformed temporary shapes can be made in a pre-determined manner.

The light-induced shape-memory functionality of the polymers was quantified by cyclic photomechanical experiments at 25 or 35 °C under stress-controlled and/or strain-controlled conditions. These cyclic experiments have been designed in analogy to those characterizing a thermally induced effect[4,18]. A typical elongation–time diagram of the grafted polymer is shown in Fig. 3, which was obtained during a cyclic photomechanical test under stress-controlled conditions. Initially, the sample is elongated to ε_{max} and the stress is kept constant. During 1.5 h of photo-crosslinking in the first cycle, the elongation stayed constant in the stretched state, indicating no relaxation of the polymer. After switching off the UV light ($\lambda > 260$ nm) and lowering the controlled stress to zero, a temporarily fixed elongation ε_u was observed. The fixed temporary shape is maintained for 3 h until UV light of $\lambda < 260$ nm is switched on for 1.5 h, activating the shape recovery of the temporarily fixed shape to nearly its original length characterized by a remaining elongation ε_p. This cycle is then repeated twice. The experiment allows the determination of the strain-fixity rate of the *N*th cycle $R_f(N) = \varepsilon_u(N)/\varepsilon_{max}$, as well as the strain-recovery rate $R_r(N) = (\varepsilon_{max} - \varepsilon_p(N))/\varepsilon_{max}$[18,19]. The strain fixity rate $R_f(N)$ describes the ability to fix the mechanical deformation that has been applied during the photo-crosslinking process. The strain recovery rate $R_r(N)$ quantifies the ability of the material to recover its permanent shape in the *N*th cycle. Similar shape-memory properties were obtained under strain-controlled conditions (Table 1). Increasing the amount of photo-crosslinker HEA-CA improves both R_f and R_r. However, increasing HEA-CA to more

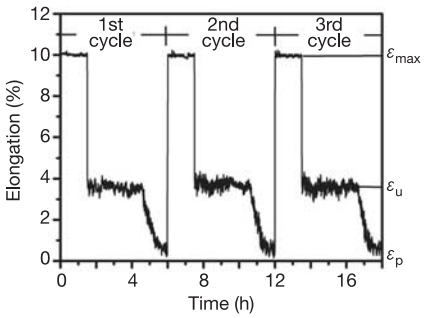

Figure 3 Cyclic photomechanical experiment on a grafted polymer BHCA (10,2,1) under stress-controlled conditions. Here $\varepsilon_{max} = 10\%$, $T = 25$ °C). ε_u is the temporarily fixed elongation, and ε_p is the remaining elongation after shape recovery.

Table 1 **Shape-memory properties of photoresponsive polymer networks at 25 °C**

Polymer type	Sample ID	ε_{max} (%)	Stress control		Strain control	
			R_f (%)	R_r (%)	R_f (%)	R_r (%)
Grafted polymer	BHCA(10,2,0.1)*	10	11	78	14	54§
	BHCA(10,2,0.25)	10	17	82	18	79§
	BHCA(10,2,0.5)	10	25	85	28	82§
	BHCA(10,2,1)	10	36	94	38	97§
	BHCA(10,2,2)	10	36	98	38	98§
	BHCA(10,2,3)	20	n.d.	n.d.	52	95§
IPN polymer	BP-SCAA†	20	20	90	33 (30)‡	98 (95)‡
	BP-SCAA†	50	15	94	20 (20)‡	95 (95)‡
	BP-SCAA†	100	n.d.	n.d.	20 (18)‡	88 (90)‡

Data from third cycle (IPN); fifth cycle (Grafted). n.d., not determined.
*Data in brackets indicate the molar co-monomer ratio (BHCA), with B = BA, H = HEMA, and CA = HEA-CA.
†IPN from BA (B) and 3.0 wt% PPG2M1000 (P) as crosslinker, loaded with 20 wt% SCAA.
‡Data in brackets were obtained at 35 °C.
§$R_r(N) = (\varepsilon_{max} - \varepsilon_p(N))/(\varepsilon_{max} - \varepsilon_p(N-1))$

than 10 mol% has no further influence on the shape-memory properties. After two cycles of UV irradiation, the clear film turned pale yellow, possibly owing to photo-Fries rearrangement[20], but no changes of shape memory properties were observed (Fig. 3). Although the extent of photoreversibility of the photoresponsive chromophores is around 40%, it is likely that partial cleavage of the photoreversible crosslinks on the microscopic level can lead to the changes of macroscopic mechanical properties and to the shape recovery.

Polymers from the IPN polymer system show an R_f of 20–33% and an R_r of more than 88%. Data obtained at 35 °C (Table 1) are not much different from those obtained at 25 °C. During the irradiation process, the temperature of the polymers does not change, indicating that heating is not the trigger of shape-memory behaviour. When the cyclic photomechanical experiment is performed at lower ε_{max} (such as 20%), higher values for R_f are obtained. Large deformation will broadly distribute the photoresponsive groups within the specimen under test and make aggregation of these functional groups difficult, thereby influencing the photo-fixing reactions. The relaxation behaviour of IPN polymer networks was investigated in control tests, in which an IPN polymer film was examined in the cyclic mechanical test under the same conditions but without applying UV light. The extent of relaxation determined from these experiments is about 2% in a test with $\varepsilon_{max} = 20\%$, and 5% for $\varepsilon_{max} = 50\%$.

Relative to thermoresponsive shape-memory polymers, the strain-recovery rate of photoresponsive shape-memory polymers is comparable, but the strain-fixity rate is much lower, because the mechanism is different. In photoresponsive polymers, the amorphous permanent network itself has long and coiled segments between two netpoints. During the programming process, the coiled segments of the chains are stretched and elongated (Fig. 1C). The strain-fixation via light irradiation is due to formation of new chemical netpoints, rather than freezing the stretched chains as in the case of thermoresponsive shape-memory polymers. The elastic contraction of the stretched chain segments accounts for the lower strain-fixity rate of light-induced shape-memory polymers. However, the unique characteristics of the photoresponsive shape-memory polymers enable shape-recovery at ambient temperatures by using remote activation, and could eliminate the temperature constraints of thermoresponsive shape-memory polymers for medical and other applications arising from external sample heating. □

Methods

Synthesis

As an example of the grafted polymer, the synthesis of BHCA(10,2,1) (see Table 1 for nomenclature) is described: a solution of 12.80 g (100 mmol) BA, 2.60 g (20 mmol) HEMA, 2.46 g (10 mmol) HEA-CA, 0.22 g (0.4 mmol) PPG2M560 and 0.05 g azo-isobutyronitril (AIBN) was polymerized between two glass sheets with a Teflon spacer of ~0.5 mm at 80 °C for 12 h. The resulting films were swollen in chloroform to remove the residual monomers. SCAA was synthesized by reacting 4-arm star-poly(ethylene glycol) ($M_n = 2{,}000$, Shearwater Polymers) with an excess of cinnamylidene acetyl chloride in dry THF solution with triethylene amine as the acid receptor.

Cyclic photomechanical and mechanical tests

These were carried out at 25 or 35 °C (selected to be $T > T_g$ and $T > T_{m,SCAA}$, the melting point of SCAA) on a Zwick-Z005, a tensile tester equipped with a 10 N load cell and a thermochamber (model 091250, Climatic Systems Ltd) controlled by a Eurotherm 902-904 unit (Eurotherm Controls Ltd). Films are cut into standard samples (ISO 527-2/1BB, length 32 mm, width 2 ± 0.2 mm). The elongation rate is 10 mm min^{-1}. For photomechanical tests, an optical system consisting of two UV lamps (30 W, Cathodeon) and an optical filter having the ability to split a light beam reaching the filter at an angle of 45° were added to this set-up. While light having wavelength $\lambda > 260$ nm is passing through the filter, light with wavelength $\lambda < 260$ nm is being reflected.

The influence of UV irradiation on the temperature of the polymer film in the Zwick thermochamber was investigated by inserting a digital thermocouple (RS Components) into the polymer film. During a 1.5 h irradiation period with UV light ($\lambda > 260$ nm or $\lambda < 260$ nm) at 25 or 35 °C, the average fluctuation of the polymer temperature is ±0.1 °C.

Received 6 December 2004; accepted 2 February 2005; doi:10.1038/nature03496.

1. Osada, Y. & Matsuda, A. Shape memory in hydrogels. *Nature* **376,** 219 (1995).
2. Liu, C. & Mather, P. T. Thermomechanical characterization of a tailored series of shape memory polymers. *J. Appl. Med. Polym.* **6,** 47–52 (2002).
3. Rousseau, I. A. & Mather, P. T. Shape memory effect exhibited by smectic-C liquid crystalline elastomers. *J. Am. Chem. Soc.* **125,** 15300–15301 (2003).
4. Lendlein, A. & Kelch, S. Shape-memory polymers. *Angew. Chem. Int. Edn Engl.* **41,** 2034–2057 (2002).
5. Wei, Z. G., Sandström, R. & Miyazaki, S. Shape-memory materials and hybrid composites for smart systems: Part I. Shape-memory materials. *J. Mater. Sci.* **33,** 3743–3762 (1998).
6. Koerner, H. *et al.* Remotely actuated polymer nanocomposites—stress-recovery of carbon-nanotube-filled thermoplastic elastomers. *Nature Mater.* **3,** 115–120 (2004).
7. Maitland, D. J. *et al.* Photothermal properties of shape memory polymer micro-actuators for treating stroke. *Lasers Surg. Med.* **30,** 1–11 (2002).
8. Eisenbach, C. D. Isomerization of aromatic azo chromophores in poly(ethyl acrylate) networks and photomechanical effect. *Polymer* **21,** 1175–1179 (1980).
9. Li, M. H. *et al.* Light-driven side-on nematic elastomer actuators. *Adv. Mater.* **15,** 569–572 (2003).
10. Finkelmann, H., Nishikawa, E., Pereira, G. G. & Warner, M. A new opto-mechanical effect in solids. *Phys. Rev. Lett.* **87,** 015501 (2001).
11. Camacho-Lopez, M., Finkelmann, H., Palffy-Muhoray, P. & Shelley, M. Fast liquid-crystal elastomer swims into the dark. *Nature Mater.* **3,** 307–310 (2004).
12. Yu, Y. L., Nakano, M. & Ikeda, T. Directed bending of a polymer film by light. *Nature* **425,** 145 (2003).
13. Ikeda, T. *et al.* Anisotropic bending and unbending behavior of azobenzene liquid-crystalline gels by light exposure. *Adv. Mater.* **15,** 201–205 (2003).
14. Suzuki, A. & Tanaka, T. Phase transition in polymer gels induced by visible light. *Nature* **346,** 345–347 (1990).
15. Juodkazis, S. *et al.* Reversible phase transitions in polymer gels induced by radiation forces. *Nature* **408,** 178–181 (2000).
16. Akabori, S. *et al.* The novel synthesis of photoreversible cyclobutanocrown ethers by the intramolecular photoaddition of α,ω-dicinnamoyl polyethylene glycol derivatives. *Bull. Chem. Soc. Jpn* **60,** 3453–3455 (1987).
17. Tanaka, H. & Honda, K. Photoreversible reactions of polymers containing cinnamylideneacetate derivatives and the model compounds. *J. Polym. Sci. Polym. Chem. Edn* **15,** 2685–2689 (1977).
18. Kim, B. K., Lee, S. Y. & Xu, M. Polyurethanes having shape memory effects. *Polymer* **37,** 5781–5793 (1996).
19. Tobushi, H., Haray, H., Yamaday, E. & Hayashi, S. Thermomechanical properties in a thin film of shape memory polymer of polyurethane series. *Smart Mater. Struct.* **5,** 483–491 (1996).
20. Haddleton, D. M., Creed, D., Griffin, A. C., Hoyle, C. E. & Venkataram, K. Photochemical crosslinking of main-chain liquid-crystalline polymers containing cinnamoyl groups. *Makromol. Chem. Rapid Commun.* **10,** 391–396 (1989).

Supplementary Information accompanies the paper on **www.nature.com/nature**.

Acknowledgements We thank the Bundesministerium für Bildung und Forschung for a BioFuture Award; H.J. is grateful for an AvH fellowship in 1999/2000.

Competing interests statement The authors declare competing financial interests: details accompany the paper on **www.nature.com/nature**.

Correspondence and requests for materials should be addressed to A.L. (Lendlein@gkss.de).

A doubling of the post-perovskite phase boundary and structure of the Earth's lowermost mantle

John W. Hernlund[1], Christine Thomas[3] & Paul J. Tackley[1,2]

[1]*Department of Earth and Space Sciences, and* [2]*Institute of Geophysics and Planetary Physics, University of California, Los Angeles, Los Angeles, California 90095-1567, USA*
[3]*Department of Earth and Ocean Sciences, University of Liverpool, Liverpool L69 3GP, UK*

The thermal structure of the Earth's lowermost mantle—the D″ layer spanning depths of ~2,600–2,900 kilometres[1]—is key to understanding the dynamical state and history of our planet. Earth's temperature profile (the geotherm) is mostly constrained by phase transitions, such as freezing at the inner-core boundary or changes in crystal structure within the solid mantle, that are detected as discontinuities in seismic wave speed and for which the pressure and temperature conditions can be constrained by